Influence of thermal annealing and magnetic field on first order magnetic transition in Pd substituted FeRh

Journal of Physics: Conference Series **200** (2010) 032038 doi:10.1088/1742-6596/200/3/032038

Influence of thermal annealing and magnetic field on first order magnetic transition in Pd substituted FeRh

Pallavi Kushwaha, Archana Lakhani, R Rawat and P Chaddah

UGC-DAE Consortium for Scientific Research
University Campus, Khandwa Road
Indore-452001, M.P, India.

E-mail: archnalakhani@csr.ernet.in

Abstract.

Influence of successive thermal annealing and magnetic field on First order antiferro (AFM) to ferromagnetic (FM) transition in the Pd substituted FeRh has been studied. With successive thermal annealing CsCl type bcc phase increases at the expense of fct (pseudo fcc) phase. Resistivity measurements do not show any transition in as-cast sample in contrast to annealed samples. AFM to FM transition temperature (T_N)is found to decrease with higher annealing temperature. With the application of magnetic field, T_N shift to lower temperature. These measurements show anomalous thermomagnetic irreversibility besides showing giant magnetoresistance across magnetic field induced first order AFM to FM transition.

75.30.Kz, 72.15.Gd

1. Introduction

Equiatomic FeRh and related system are of interest due to the observation of giant magnetocaloric effect, elastocaloric effect, magnetoresistance (MR), magnetostriction etc. [1, 2, 3]. In its ordered bcc crystal structure, three magnetic phases (para (PM), ferro (FM) and antiferromagnetic (AFM)) appear with temperature in quick succession. A FM state appears around $\approx 650K$ (T_C) and at low temperature it transforms to an AFM (type-II) state ($T_N \approx 350K$) through a first order transition. In the FM region, magnetic moments on Fe and Rh are $3.2\mu_B$ and $0.9\mu_B$ respectively whereas in the AFM region there is no appreciable moment on Rh [4, 5]. The FM to AFM transition is very sensitive to the doping and the heat treatment. In fact the magnetic behavior of these systems depend strongly upon crystal structure which can be modified by annealing, pressure, stress etc. A structural phase transition from bcc to tetragonal structure has been observed [6] with pressure. Stress induced by filing introduces a bcc to fcc transition [3], whereas structure of FeRh nanoparticles is found to be fcc [7]. Therefore to investigate the role of various factors it is necessary to carry out the systematic studies as a function of one of these parameters keeping others constant. Here we report our study of thermal annealing effect on the structure and the first order AFM to FM transition in $Fe_{49}(Rh_{0.93}Pd_{0.07})_{51}$. With Pd doping T_N can be shifted to the lowest temperature and is expected to be minimum around this composition. To take care of sensitivity of T_N

on composition, samples from a single button of as cast sample are used for all the thermal treatment.

2. Experimental Details

The compound $Fe_{49}(Rh_{1-x}Pd_x)_{51}$ with $x = 0.07$ is prepared by arc melting the constituent elements of purity better than 99.9% under high purity argon atmosphere. Small pieces, cut from the same as cast ingot (sample-A), were wrapped in Tantalum foil and sealed in a quartz tube in $\approx 10^{-6} torr$ of vacuum and annealed at 800^0C (sample-B) and 900^0C (sample-C) for 48 and 20 hours respectively followed by quenching in ice water. For crystal structure analysis and the other phase detection, X-ray diffraction (XRD) has been performed on polished surface of the ingot. The resistivity (ρ) and longitudinal MR ($= \{\rho(H) - \rho(0)\}/\rho(0)$) measurements were carried out by standard four-probe technique using a home made resistivity setup with 8 Tesla superconducting magnet system (Oxford Instruments Inc., UK).

3. Results and discussion

Figure 1 shows the XRD pattern for all the samples annealed at different temperature. All patterns were fitted using Rietvelt refinement program DBWS486 and the best fit is shown as a line graph in the same figure. We tried to fit our XRD pattern assuming the presence of bcc and fcc phases, however fit is found to be unsatisfactory. Then we assumed the structure of secondary phase as fct with space group $P4/mmm$ (Fe at 1a and 1c Wyckoff sites, Rh / Pd at 2e). As can be seen in figure 1, all the observed peaks in the XRD pattern of sample-A can now be indexed with this combination. The peaks corresponding to fct and bcc phases are marked by star(*) and vertical lines (|) respectively. The lattice parameter and phase fractions obtained from the refinement are listed in Table 1. In case of sample-B a small peak corresponding to elemental Fe is highlighted as the inset of figure 1. Therefore the estimated phase fractions obtained from fitting may not be accurate in this case. Except sample-B, obtained lattice parameter of fct phase are in close agreement with the 'a' parameter of fcc phase [9]. With increasing annealing temperature CsCl type bcc phase increases from $\approx 41\%$ (sample-A) to $\approx 86\%$ (sample-C).

ρ-T curve in figure 2 shows the effect of structural transformation from fct to bcc structure on the FM to AFM transition. For sample-A, ρ does not show any signature of AFM-FM transition but the difference between ρ value during cooling and heating cycle is noticeable over entire temperature range (shown in the inset of figure 2 [a]). Sample-B as well as sample-C, both show a clear signature of FM to AFM transition as a sharp increase in ρ with decreasing temperature. During warming, the reverse transition occurs at higher temperature resulting in a hysteresis which is a signature of first order transition. The transition temperature (taken as the average value of the temperature corresponding to minmum of first derivative of ρ curves during cooling and warming) are found to be $\approx 263K$ and $\approx 211K$ for sample-B and C, respectively. With higher annealing temperature the ρ jump ($\Delta\rho$) across AFM-FM transition and the hysteresis width (H_W; difference between the transition temperature observed during cooling and warming) increases, whereas the FM to AFM transition temperature decreases keeping transition width

Table 1. Variation of lattice parameters, phase fraction, transition temperature (T_N), transition width (T_W), hysteresis width (H_W) and resistivity jump ($\Delta\rho$) at T_N for samples -A, B and C.

Sample	bcc 'a'	fct 'a', 'c'	bcc phase fraction	T_N	T_W	H_W	$\Delta\rho$ at T_N
Sample-A	$3.003\mathring{A}$	$3.752\mathring{A}$, $3.748\mathring{A}$	41%	–	–	–	–
Sample-B	$2.988\mathring{A}$	$3.859\mathring{A}$, $3.856\mathring{A}$	46%	$263K$	$55K$	$15K$	$25\mu\Omega$ cm
Sample-C	$2.997\mathring{A}$	$3.763\mathring{A}$, $3.722\mathring{A}$	86%	$211K$	$55K$	$20K$	$50\mu\Omega$ cm

(T_W) constant (see Table-1). The increase in the ρ jump with higher annealing temperature can be attributed to the increased bcc phase fraction, which shows the first order AFM-FM transition. Besides this in case of sample-B, zero field ρ is found to be higher at room temperature during warming compared to initial resistivity before cooling. This suggest an incomplete AFM to FM transformation and the presence of superheated AFM state during warming which is further verified by isothermal MR measurements discussed in following sections.

Influence of the magnetic field on AFM-FM transition temperature is studied by measuring ρ in the presence of 8 T magnetic field under different protocols. For these measurements 8 T magnetic field is applied isothermally after sample is cooled under zero field to 5 K and then ρ is measured during warming (ZFCW), subsequent cooling (FCC) and again warming (FCW) in the presence of 8 T magnetic field. For sample-B, T_N is shifted to the lower temperature and there is no difference between the ZFCW and FCW curve. In contrast to sample-B, sample-C shows absence of FM to AFM transition during field cooling (FCC) giving rise to a large thermomagnetic irreversibility between ZFCW and FCW curves. These irreversibilities are similar to that observed in Co doped Mn_2Sb [10]. In analogy to this system, difference between ZFCW and FC curves at low temperature for sample-C shows that as T_N is shifted to lower temperature, the FM-AFM transformation is hindered due to the slow dynamics of the transition. Whereas, in case of sample-B, no such thermomagnetic irreversibility has been observed as T_N is higher even in the presence of 8 Tesla magnetic field.

Figure 3 shows the results of MR measurement for Sample-B at 300K (slightly above T_N) and 100K (below T_N). For these measurements magnetic field is applied isothermally at room temperature after completing the warming cycle of zero field resistivity. At 300K, where sample is almost in the FM state, we observe a large MR ($\approx 27\%$). Though there is no sharp change in MR, the hysteresis in the envelope curve suggests a gradual AFM-FM transition. Another interesting feature of this MR curve is that the virgin curve is lying outside the envelope curve and the zero field resistivity is different before and after field cycling. It has been shown in the context of Co doped Mn_2Sb that for a negative slope of T_N line in the H-T space, magnetic

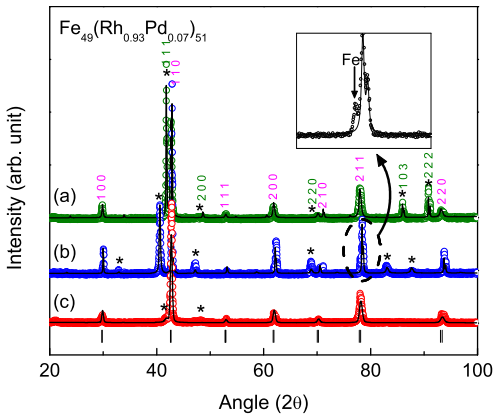

Figure 1. X-ray diffraction pattern for [a] sample-A (as cast) [b] sample-B (annealed at 800^0C for 48 hours) [c] sample-C (900^0C for 20 hours). Peaks marked by stars (*) and vertical lines (|) correspond to fct and bcc structure respectively. Peak corresponding to element Fe is highlighted in the inset by arrow.

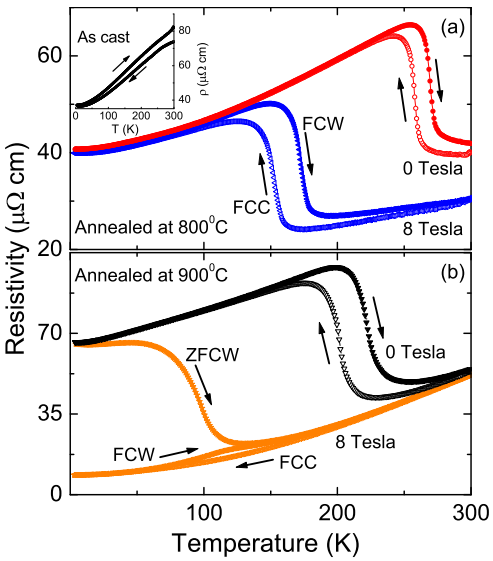

Figure 2. ρ vs. T at 0 and 8 Tesla magnetic field for (a) sample-B (b) sample-C. Inset in (a) shows zero field ρ-T curve for sample-A. See text for details.

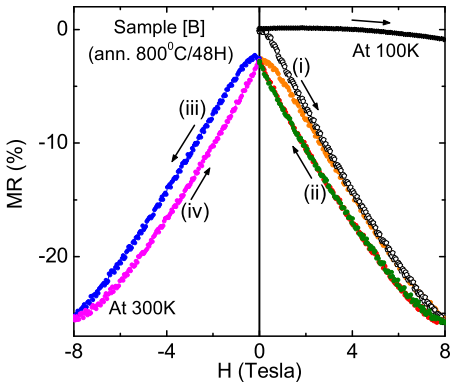

Figure 3. MR vs. H for sample-B.

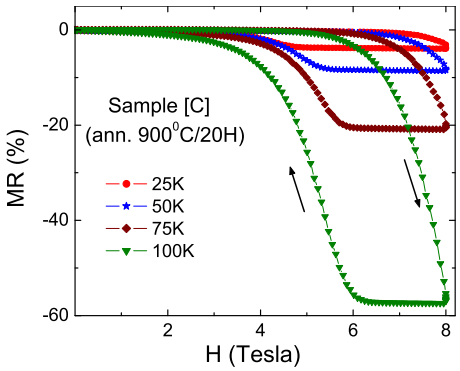

Figure 4. MR vs. H for sample-C.

states are different before and after field cycling if and only if the measurement temperature is reached by warming [10]. At 100K, MR is negligible ($\approx 1\%$) indicating a stable AFM state up to 8 Tesla magnetic field, which is consistent with our ρ-T measurements shown in figure 2[a].

Sample-C shows a giant MR ($\approx 60\%$ at 100K) associated with field induced AFM to FM transition as shown in figure 4. 8 T magnetic field is not sufficient to complete the AFM to FM transformation even at 100K is evident from the non overlapping region during warming and cooling. With decreasing temperature, the magnitude of MR decreases as the magnetic field required for the AFM-FM transition further increases resulting in smaller AFM-FM transformation. This is consistent with figure 2(b) where we do not observe any difference between zero field and 8 T ρ (ZFCW) at 5 K indicating a almost homogenous AFM state at 8 Tesla for zero field cooled sample. Whereas cooling in presence of 8 T results in almost homogenous FM phase at 5K. This suggest that at low temperature FM-AFM transition is hindered on experimental time scale.

4. Conclusions

Influence of the thermal annealing has been studied in Pd doped polycrystalline FeRh. Observed peaks in the as-cast sample shows the presence of bcc and fct (pseudo fcc) phase in contrast to earlier reports where bcc and fcc phase is reported. With successive annealing bcc phase increase at the expense of fct phase. The consequences of increased bcc fraction are manifested in the appearance of first order FM to AFM transition and its shift toward lower temperature. In field ρ measurement reveal anomalous thermomagnetic irreversibility when the transition temperature is shifted to lower temperature. Giant MR ($\approx 60\%$ at 100K for sample-C) has been observed across a field induced AFM-FM transition.

5. Acknowledgements

We acknowledge N. P. Lalla, R. J. Choudhary and Suresh Baradwaj for XRD measurements. V. Sathe is acknowledged for his help in XRD data refinement.

[1] Algarabel P A, Ibarra M R, Marquina C and Moral A del 1995 *Appl. Phys. Lett.***66** 3061.
[2] Annaorazov M P, Nikitin S A, Tyurin A L, Asatryan K A and Dovletov A Kh, 1996 *J. Appl. Phys.* **79** 1689.
[3] Ibarra M R and Algarabel P A, 1994 *Phys. Rev. B* **50** 4196.
[4] Moruzzi V L and Marcus P M 1992 *Phys. Rev. B* **46** 2864.
[5] Shirane G, Chen C W, Flinn P A, and Nathans R 1963 *J. Appl. Phys.* **33** 1044.
[6] Rajagopalan M 2005 *Inte. J. Mod. Phy. B* **19** 3389.
[7] Hernando A et al. 1998 *Phys. Rev. B* **58** 5181.
[8] Nguyen H Loc et al. 2005 *J. Mater. Chem.* **15** 5136.
[9] Kouvel J S and Hartelius C C 1962 *J. Appl. Phys.* **33** 1343.
[10] Kushwaha Pallavi, Rawat R and Chaddah P 2008 *J. Phys.: Condens. Matter* **20** 022204.